Journal of Hydrology 497 (2013) 24–36

Contents lists available at SciVerse ScienceDirect

Journal of Hydrology

journal homepage: www.elsevier.com/locate/jhydrol

A graphical method to study suspended sediment dynamics during flood events in the Wadi Sebdou, NW Algeria (1973–2004)

Abdesselam Megnounif [a], Abdelali Terfous [b], Sylvain Ouillon [c,d,*]

[a] Laboratoire EOLE, Université Aboubakr Belkaid, BP 230, Tlemcen 13000, Algeria
[b] Design Engineering Laboratory, LGECO, ERESA, INSA Graduate School of Science and Technology, 24 bd de la victoire, 67084 Strasbourg, France
[c] Université de Toulouse, UPS (OMP), IRD, UMR 5566 LEGOS, 14 av. Edouard Belin, 31400 Toulouse, France
[d] University of Science and Technology of Hanoi (USTH), 18 Hoang Quoc Viet, Cau Giay, Hanoi, Viet Nam

ARTICLE INFO

Article history:
Received 8 October 2012
Received in revised form 21 February 2013
Accepted 11 May 2013
Available online 30 May 2013
This manuscript was handled by Konstantine P. Georgakakos, Editor-in-Chief, with the assistance of Ehab A. Meselhe, Associate Editor

Keywords:
Hysteresis
Suspended sediment concentration
Semiarid watershed
Flood
Wadi
Algeria

SUMMARY

Small sub-basins are numerous in Mediterranean area and global sedimentary budgets cannot be obtained without a detailed understanding of the hydroclimatic processes that govern sediment fluxes in these small river systems. In this study, the shape of the relationship between sediment concentration (*C*) and water discharge (*Q*) during flood events of a 31-years period (1973–2004) was analyzed at the outlet of the Wadi Sebdou basin (256 km^2) in northwest Algeria, using a new graphical analysis method based on features of hysteresis loops. Each flood was decomposed as successive stages – each of which being characterized by a sediment rating curve – and used to quantify the contribution of diverse sediment sources within the basin. Seven common classes of hydrological events (single valued and six hysteresis loops: clockwise, counter-clockwise, eight-shaped, single valued plus one loop, either clockwise or counter-clockwise, and single valued plus at least two loops) were explored. Sediment supply from locally derived sources (or "base load") was high and reached 77% of total sediment yield for the study period, and was attributed to weathering of bed material or gullies. The remainder portion was derived from hill-slopes, re-suspension of fresh fine deposits in the river bed, or bank collapse. The ratio of suspended sediment load derived from active sediment source varies considerably from one flood to another depending on many factors, such as seasonality and antecedent type of flood. The simpler floods were the most frequent ones but produced less sediment. The most frequent floods were clockwise or anticlockwise (52% of floods) but brought only 34% of the total sediment flux. The 18% of the most complex floods (single valued plus at least two loops) produced more than 53% of the sediments, mainly supplied by base load (84%). Intra-annual variability was very high. Over 31-years, the five biggest floods cumulated 64% of the total sediment flux and were of three classes, the most complex floods being dominant. The largest contribution occurred during one single 33-days long hydrological event with complex form which represented 26% of the total sediment flux. Apart from the five biggest flood events, the base load represented 53%. The biggest floods favour base load as compared to the smallest ones.

1. Introduction

Sediment transfer via rivers is a key issue in studying global water and element cycles. In the Maghreb area, possessing only scarce water resources, the major damage is associated with the loss of alluvial sediments from the catchment and subsequent dam siltation. The mean annual suspended sediment flux in the Maghreb rivers was estimated to be 254 millions of metric tonnes (Probst and Amiotte-Suchet, 1992). Between 37% and 98% settles in reservoirs (Ghorbal and Claude, 1977). These deposits contribute to about 2–5% of the yearly loss of water storage capacity (Kassoul et al., 1997). Thus, to implement a better water resources management strategy, there is a pressing need to understand the genesis and dynamics of sediments in this area.

Currently discharge and suspended sediment concentration are the requisite data for calculating suspended sediment fluxes. However, the amount of sediment crossing a stream station at a given time is a function of a complicated set of active and passive forces acting on the drainage basin which are governed by many factors such as basin morphology and lithological formations; antecedent moisture of catchment soils; precipitation intensity and areal distribution; seasonal variations in vegetation cover; deforestation and land use; spatial and temporal storage – mobilization – depletion

* Corresponding author at: Institut de Recherche pour le Développement, University of Science and Technology of Hanoi (USTH), 18 Hoang Quoc Viet, Cau Giay, Hanoi, Viet Nam. Tel.: +84 125 813 47 45.

E-mail addresses: megnounif_aslam@yahoo.fr (A. Megnounif), abdelali.terfous@insa-strasbourg.fr (A. Terfous), sylvain.ouillon@ird.fr, sylvain.ouillon@legos.obs-mip.fr (S. Ouillon).

0022-1694/$ - see front matter © 2013 Elsevier B.V. All rights reserved.
http://dx.doi.org/10.1016/j.jhydrol.2013.05.029

processes of available sediment; sediment travel rates and distances from the areas of different sediment sources. The potential mix and interrelations of these factors result in so-called hysteresis effects in the relationships between river flow and suspended sediment concentration (Williams, 1989). Studies have identified sediment sources by analysing hysteresis loops of discharge–suspended sediment relations at both a single-event and seasonal scales, for large and small basins with contrasting climatic and hydrological characteristics (Asselman, 1999; Picouet et al., 2001; Jansson, 2002; Lecce et al., 2005; Bača, 2008; Gellis, 2013).

The high sediment transport efficiency exerted by Algerian rivers (Colombani et al., 1984; Bourouba, 1998) has encouraged many authors to investigate suspended sediment transfer in this area. During the last decade, several works have concentrated on evaluating budgets and analysing spatial and temporal variability of sediment yields (Megnounif et al., 2003; Achite and Meddi, 2005; Achite and Ouillon, 2007; Ghenim et al., 2007, 2008). Given such problems and in order to determine the service life of dams and to implement a better water resources management strategy, research on sediment dynamics emphasises the need for a better understanding of variations in the erosion, deposition, and storage dynamics of sediment in a variety of catchments and rivers. In this context, a number of studies have utilized discharge-suspended sediment concentration relations to gain more comprehensive understanding of drainage basin processes (Terfous et al., 2001; Benkhaled and Remini, 2003b; Khanchoul and Jansson, 2008).

In this paper, a detailed analysis of the hysteresis loops exhibited by discharge-suspended sediment relationship was undertaken to assess temporary sediment storage and budget components through individual flood events. The study was conducted in Wadi Sebdou or Upper Tafna basin in northwest Algeria (256 km^2). The Upper Tafna contributes to the silting of the Beni-Bahdel dam commissioned in 1946. The storage capacity was initially 63 millions of cubic metres and was estimated to be 54.8 millions of cubic metres in 1994 due to siltation (Djeziri, 1998). The goal is to examine suspended sediment transport, erosion and deposition in the Wadi Sebdou system over the 31-years period (September 1973–August 2004). A new graphical method was tested to distinguish the different origins of particles within flood events. The dynamic of sediment throughout individual flood events and their impacts on sediment budget at seasonal and inter-annual time scales were analyzed. The seasonal variability and intra-annual variability of flood types were particularly detailed.

2. Study area and methods

2.1. Study area: the Wadi Sebdou

2.1.1. Main characteristics

The catchment is mainly rural with a mix of arable and pastoral farming in lowlands and pastures with low-density sheep grazing in the uplands. The upper reaches of the river flow maximum at altitude of 1400 m and the tributary streams join the river on the Sebdou plain (900 m). About 49% of the total Wadi Sebdou basin surface has slopes exceeding 25%.

The gauging Beni-Bahdel station (latitude: 34°41.85′ N; longitude: 01°27.19′ W; elevation: 665 m) is located at the outlet of the basin and approximately 1000 m upstream the inlet of the dam (Fig. 1).

2.1.2. Climate, rainfall and runoff

The climate of the study area is Mediterranean. The mean annual temperature is 17.2 °C (September 1955–August 1992). January is the coldest month with mean temperatures of 8.3 °C; the maximum monthly mean, 28.4 °C, was recorded in August. The annual mean potential evaporation is 1390 mm (Bouanani, 2004).

The topographic differences across the catchment yield a rainfall spatial variability. The mean annual precipitation varies between 538 mm on the north-facing hill-slopes and 278 mm on those to the south or in the interior plains characterized by strong thermal variations and excessive summer dryness dominated by the Saharan Winds (Megnounif et al., 1999). Saharan Winds – Sirocco – carry large quantities of fine grained sediments and occur with an average of 7 days per year. Rainfall gauged near outlet of the Wadi Sebdou catchment provided mean annual value of 466 mm over the period September 1939–August 2004 while the mean annual discharge was 1.71 m^3 s^{-1}. Rain mainly occurs in autumn and spring. Rainfall showed a high inter-annual variability with a coefficient of variation – i.e. standard deviation divided by the mean – of 31%, water discharge being more irregular than rainfall (coefficient of variation of 63%).

In the 1970s, rainfall and discharge began to decrease. The diminution of rainfall by 23.7% between the period 1939–1975 (526 mm) and the period 1975–2004 (401 mm) induced a decrease by 55% of the yearly volume discharged by Wadi Sebdou in 1975–2004 as compared to 1939–1975. A similar variability was observed on other Algerian basins such as Wadi Abd's (Achite and Ouillon, 2007).

The repartition of daily rains over the period September 1982–August 2009 showed that the time duration without rain valued of 84%. Days having rain intensity comprised between 10 and 30 mm, which corresponded in average to 10 days per year, contributed with 43% of total annual rainfalls. Almost 25% of the annual rainfall occurred with intensity exceeding 30 mm per day during, in average, 2 days per year. High-intensity rainstorms may reach 140 mm in 24 h.

2.1.3. Hydrological and suspended sediment data

Water flows and suspended sediment concentrations were provided by the National Agency of Hydrologic Resources [ANRH], responsible for gauging stations and measurements in Algeria (http://www.anrh.dz). The protocol of suspended sediment concentration sampling is the same in the Sebdou Wadi than in other rivers of Algeria (e.g. Terfous et al., 2001; Benkhaled and Remini, 2003a,b; Achite and Ouillon, 2007).

River discharge (Q, in m^3 s^{-1}) was obtained from the water level continuously measured by a limnimetric ladder and float water level recorder, using a rating curve. During flow measurement, water was manually sampled using a 1 L dip sample. One or two samples were measured at the edge of the Wadi. The number of samples was adapted to the hydrological regime. The sampling rate depended on the flow event, every other day or, during floods, at high rates (up to every 30 min).

The samples were collected and subjected to standard concentration analysis by filtration. The ANRH protocol is as follows: suspended sediments are defined as the portion of total solids retained by a fiberglass membrane (Whatman GF/F) of porosity 0.6 μm. The sediment collected was weighed after being dried at 105 °C for 24 h. The difference in weight of the filter before and after filtration enabled the suspended sediment concentration to be calculated based on the volume of water filtered (C, in g L^{-1}).

During the period of investigation (September 1973–August 2004), water was always present in the Wadi. According to the terminology used in ecological studies in Uys and O'Keeffe (1997), the flow regime of the Wadi Sebdou has been perennial. Peak discharge exceeded 100 m^3 s^{-1} and occurred mainly in spring or in early autumn. The lowest discharges were recorded in the summer.

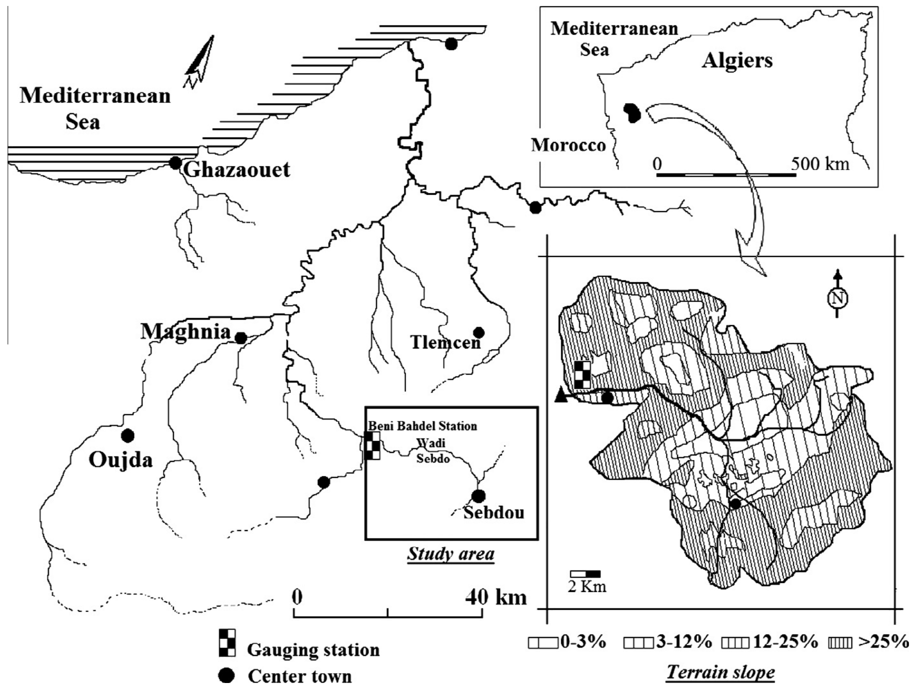

Fig. 1. Location of the Wadi Sebdou basin and terrain slopes.

2.2. Criteria for flood selection

The study was based on the examination of instantaneous measurements of the water flows, $Q(t_j)$, and suspended sediment concentration, $C(t_j)$, measured at the time t_j (in s) spanning the interval [0, T] of the flood event under consideration. During the period September 1973–August 2004, it allowed the identification of 131 high discharge events which fitted the following criteria: (i) Q exceeded the annual mean flow of the year under consideration or the peak C was higher than 1 g L^{-1} and (ii) an event was defined as starting at the time when Q exceeded the annual mean flow or C exceeded 0.2 g L^{-1}, and was defined as ending when Q and/or C decreased below these levels. The main characteristics of these flood events are summarized in Table 1. A total of 2112 paired (C, Q) readings were recorded during 131 flood events.

2.3. Suspended sediment yield

At the flood event scale, the total suspended sediment yield crossing the outlet (Y_S in tonnes) is given by:

$$Y_S = Y_{S1} + Y_{S2} = \int_{t=0}^{T} C(t)Q(t)dt \approx \sum_{j=0}^{N} \left(\frac{C_j Q_j + C_{j+1} Q_{j+1}}{2} \right) (t_{j+1} - t_j) \times 10^{-3} \quad (1)$$

where Q_j (in $m^3\ s^{-1}$) and C_j (in g L^{-1}) denote respectively discharge and sediment concentration, respectively, measured at the time t_j when the entire flood event is divided in N periods corresponding to (N + 1) samplings. Y_{S1} results from the erosive power of river flow and represents the sediment production from the stream channel network, by weathering of bed materials or gullies, and can be considered as base load. Y_{S2} represents the supply of new sediment sources that become available in the river basin (Roehl, 1962; Gregory and Walling, 1973; Robinson, 1977). This part is function of sediment availability within the basin where the wash-load material from hill-slopes, bank caving and re-suspension of fresh deposits in the hydrographical network are the main constituents.

2.4. Hysteresis

Hysteresis loop is observed when an activity and an energy source are non-synchronous during an individual cycle. Graphical proprieties of hysteresis loops are widely used in modelling numerous phenomena in engineering applications, such as: temperature, pressure, chemical reaction, rheological models, and earthquake. This approach is considered as a powerful tool to use in various hydrological problems. Currently, most investigations have examined features of hysteresis loops to gain a more comprehensive understanding on active sediment sources within the basin (Heidel, 1956; Klein, 1984; de Boer and Campbell, 1989; Williams, 1989; Hudson, 2003; Seeger et al., 2004; Fang et al., 2011).

Systematic exploration of possible C–Q relationships concluded that there are seven common classes of hysteresis loops: one single valued and six hysteresis loops: clockwise, counter-clockwise, eight-shaped, single valued plus one loop, either clockwise or counter-clockwise, and single valued plus at least two loops.

In this study, floods were decomposed in successive stages, and the form of the hysteresis of each flood was used to identify and quantify sediment sources. Successive (C, Q) data were considered as comprising a single "stage" if they were significantly correlated (Achite and Ouillon, 2007). A single stage describes a separate phase of sediment yield. A specific rating curve is defined per single stage. Amongst the 131 flood events, each single stage of the C–Q relationship was identified by the paired (i, k) and expressed by the function $C_k^i(t_j) = f_{ik}(Q_j)$, where i (i = I–VII) refers to the class of the loop, k is the number of the stage as depicted in Fig. 2, and t_j is the time of sampling. The form of the hysteresis of each flood was used to identify sediment sources. So, the decomposition of the hysteresis by a series of stages enabled us to: (1) elucidate the relationship between C–Q hysteresis types and sediment sources within the river basin, using models and field examples;

Table 1
Main hydrological and sedimentological data of recorded floods per class: *F*, seasonal frequency of flood event of a given class; *T*, time duration of flood event (in days); $\bar{C}$, mean sediment concentration throughout flood events; *R*, runoff (in hm^3); Sediment yield (Y_S; Y_{S1} in $10^3 \times$ tonnes); M.S., mean slope of the sediment rating curve estimating base load.

Class	Season	F	T	$\bar{C}$	R	Y_S	Y_{S1}	Y_{S1}/Y_S (%)	M.S.
I	Autumn	4/7	11.2	3.4	4.5	15.4	15.4	100	3.4
	Winter	1/7	6.0	9.0	0.3	2.7	2.7	100	28.41
	Spring	2/7	14.2	4.1	1.6	6.4	6.4	100	4.9
	Summer								
	Total		31.3	3.8	6.4	24.5	24.5	100	11.7
II	Autumn	14/37	62.1	18.6	19.0	353.6	219.7	62	1.47
	Winter	16/37	72.7	1.8	18.5	33.4	17.9	54	0.37
	Spring	5/37	30.3	3.1	7.1	22.0	4.6	21	0.42
	Summer	2/37	12.0	5.1	0.8	4.1	1.5	36	2.60
	Total		177.0	9.1	45.4	413.1	243.7	59	0.916
III	Autumn	13/31	29.4	22.29	8.46	188.48	163.66	87	1.50
	Winter	5/31	25.6	0.7	5.3	3.7	1.1	30	0.21
	Spring	7/31	43.2	6.0	6.8	40.9	20.5	50	1.29
	Summer	6/31	21.3	38.8	7.5	292.8	283.6	97	1.65
	Total		119.4	18.7	28.2	525.8	468.9	89	0.916
IV	Autumn	11/23	61.4	7.6	11.1	84.6	61.4	73	1.02
	Winter	6/23	39.9	2.4	15.4	37.5	14.5	39	0.26
	Spring	5/23	39.3	4.1	20.2	83.2	31.5	38	0.22
	Summer	1/23	4.0	6.7	0.2	1.3	1.1	84	11.04
	Total		144.7	4.4	46.9	206.7	108.5	52	1.08
V	Autumn	1/4	2.8	4.53	0.99	4.50	2.48	55	0.123
	Winter	2/4	17.3	1.89	7.9	14.9	10.3	70	0.334
	Spring	1/4	38	2.81	8.1	22.7	6.2	27	0.142
	Summer								
	Total		58.0	2.5	16.9	42.0	19.0	45	0.23
VI	Autumn	2/5	3.8	8.11	0.5	4.1	3.9	96	2.38
	Winter	2/5	11.8	0.86	1.2	1.0	0.9	86	0.25
	Spring								
	Summer	1/5	1.2	22.64	2.1	48.5	5.3	11	1.29
	Total		16.8	13.90	3.9	53.6	10.2	19	1.31
VII	Autumn	6/24	34.1	27.4	13.7	376.1	354.8	94	9.48
	Winter	7/24	158.8	0.6	69.5	42.7	24.3	57	0.30
	Spring	8/24	120.2	8.0	99.6	791.8	675.6	85	0.10
	Summer	3/24	20.7	10.1	23.3	234.6	163.5	70	0.16
	Total		333.9	7.011	206.1	1445.1	1218.2	84	2.51
All classes	Autumn	51/131	204.7	17.6	58.3	1026.8	821.4	80	3.08
	Winter	39/131	332.1	1.2	118.1	135.9	71.7	53	1.03
	Spring	28/131	285.1	6.7	143.3	967.0	744.8	77	0.83
	Summer	13/131	59.2	17.1	34.0	581.2	455.0	78	2.15
	Total		881.1		353.7	2710.9	2093.0	77	1.89

(2) provide a simple graphical description for each type; and (3) estimate the contribution of Y_{S1} and Y_{S2} components.

2.4.1. Class I: single-valued line

Class I flood events show one single stage, during which suspended load increases and decreases in direct synchronization with water discharge, leading to a rating curve (Fig. 2, Class I). The curve is linear when the rate of increase or decrease does not depend on water discharge. A single-value curve suggests a strong dependence of suspended sediment concentration on water discharge and is associated with an uninterrupted supply throughout the flood (Williams, 1989). It depends more on the entrainment of bed material of the channel than on the supply of hillslope sediments (Walling and Webb, 1982; Probst and Bazerbachi, 1986; Hudson, 2003).

The lonely "single stage" of this hydrological event is expressed by function $C_1^I(t_j) = f_{I1}(Q_j)$. So, $Y_S \approx Y_{S1}$, and the suspended sediment yield supplied to the outlet can be estimated by:

$$Y_{S1} = \int_{t=0}^{T} C_1^I(t)Q(t)dt \approx \sum_{j=0}^{N}\left(\frac{f_{I1}(Q_j)Q_j + f_{I1}(Q_{j+1})Q_{j+1}}{2}\right)(t_{j+1} - t_j) \times 10^{-3} \quad (2)$$

2.4.2. Class II: clockwise loop

This form is exhibited when the C/Q ratio is always higher at the rising limb than at the falling limb (Fig. 2, Class II). Clockwise loops have often been attributed to depletion of available sediment in the catchment or in the stream channel (Peart and Walling, 1982). The 1st and 2nd stages involve the rising limb of the hydrograph. At the start of flood event low energy flow is sufficient to evacuate the majority of available sediment in the catchment or in the stream channel. The first phase of such C–Q relationship (see Fig. 2, Class II (b)), characterized by a sharp increase in C with increasing Q, can be attributed to erosion of temporarily stored sediments at the beginning of the flood (Walling and Webb,

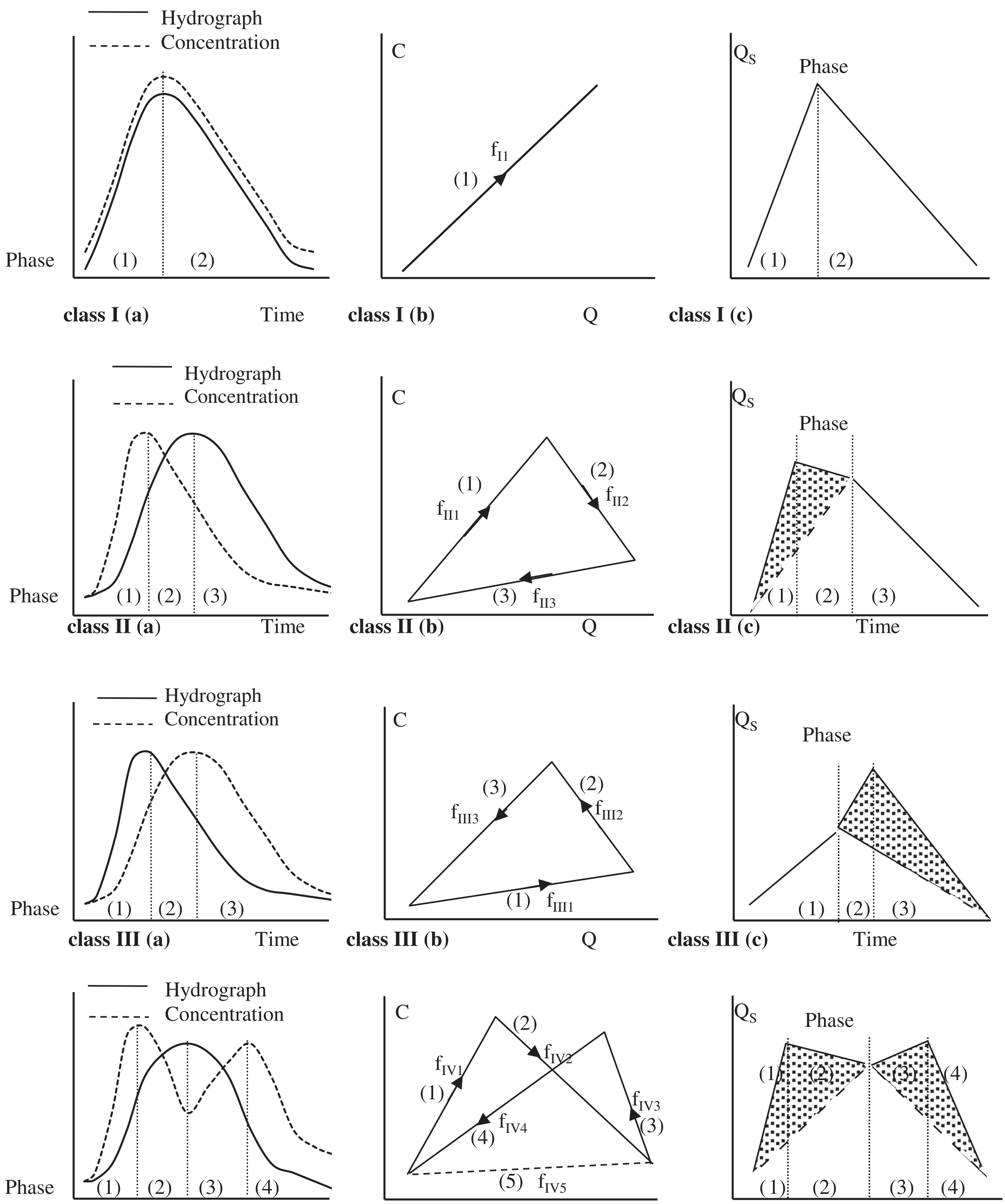

Fig. 2. Common relationships between suspended sediment concentration (C) and discharge (Q); identification of successive stages of a flood event and schematic diagram explaining evaluation of the two components: base load (Y_{S1}) and supply of new sediment sources, available in the river basin (Y_{S2}).

1981) or to the wash-load transported by the first surface runoff (Rovira and Batalla, 2006). The second phase, characterized by a decrease in C with substantial increase in Q, corresponds to sediment depletion in the channel system. The third phase is characterized by a decrease in C with decreasing energy. The maximum of river capacity corresponds to the maximum erosive power of flow. Thus we can consider that the majority of unconsolidated sediments are evacuated during the rising limb of the hydrograph inducing a depletion of the Y_{S2} component.

Walling and Webb (1982) separated the flood-flow (quick-flow) component from the delayed flow by constructing a straight line with an upward slope. The sediments sampled during the delayed flows were assumed to be derived from the channel network and correspond to the last "single stage" of the hydrograph (Fig. 2, Class II (b-3)), expressed by the function $C_3^{II}(t_j) = f_{II3}(Q_j)$. This function can be extended to the previous (1) and (2) phases and allow identifying the curve presented by dotted line (Fig. 2, Class II (c)) which separates the Y_{S1} and Y_{S2} components. Hence, the base load, i.e. Y_{S1}

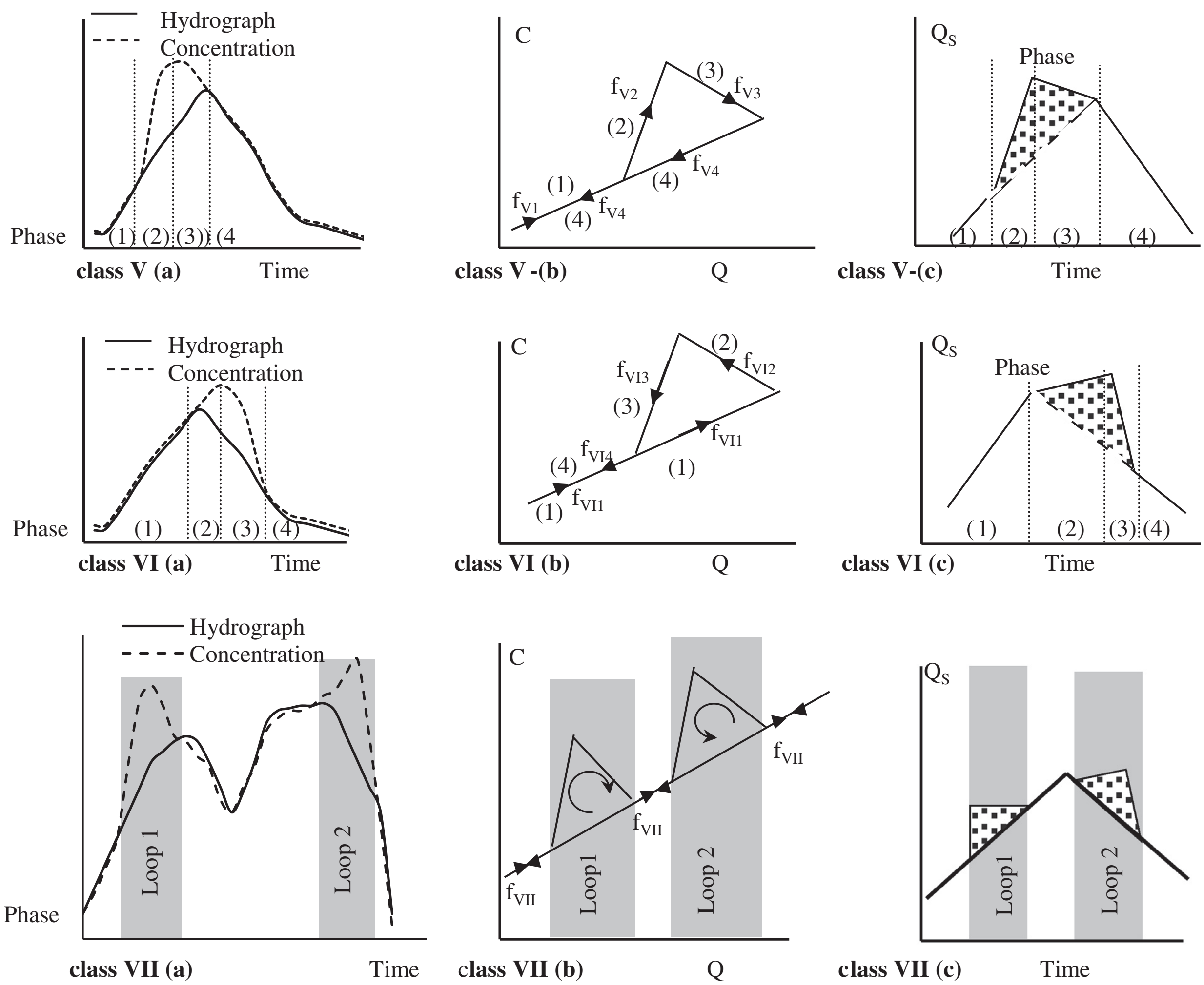

Fig. 2 (*continued*)

component can be estimated by the equation obtained from Eq. (2) with f_{II3} replacing f_{I1}. Graphically, Y_{S2} corresponds to the grey area reported in Fig. 2, Class II (c).

2.4.3. Class III: counter-clockwise loop

Similar to Class II, counter-clockwise hysteresis exhibits three distinct phases (Fig. 2, Class III). In this case, new sediment sources become available for transport during the falling limb of the hydrograph. According to Williams (1989), the counter-clockwise loop results of at least one of three causes: (i) the sediment wave which travels slower than the discharge wave; (ii) the high soil erodibility in conjunction with prolonged erosion during the rainfall episode, which caused severe and prolonged sediment erosion; and (iii) the seasonal variability of rainfall distribution, since "a minor precipitation event occurring after the major event provides additional matters from runoff-derived sources, or because the sediments are likely derived from the distal portions of the basin". Bank caving events that occur on the receding limb of the hydrograph can also infer counter-clockwise hysteresis (Asselman, 1999; Hudson, 2003). The Y_{S1} component is estimated by the equation obtained from Eq. (2) with f_{III1} replacing f_{I1}.

2.4.4. Class IV: figure eight

Eight-shaped hysteresis denotes that the ratio C/Q during the rising limb is higher than that during the falling limb over one range of Q values, and that the reverse is true for another range of Q values (Williams, 1989). Figure eight combines parts of Class II (clockwise loop) and Class III (counter-clockwise loop) hysteresis. An example is given in Fig. 2, Class IV: during the first stage, the rate of increase of C is higher than that of Q. Post-peak sediment availability and transport are high and concentration decreases slowly with increasing water discharge (second stage). The first and second stages represent the beginning of clockwise hysteresis. At the end of the second phase, river flow begins to decrease. In the third stage, new sediment sources become available for transport, and C peaks on the falling limb. The fourth stage corresponds to sediment depletion in the channel system. The third and the fourth stages produced a counter-clockwise hysteresis. Eight-shaped hysteresis can be understood as a sequence of contribution of distinct sediment sources. The initial partial clockwise hysteresis is caused by sediment depletion in the channel system or by flushing of sediments at the beginning of surface runoff. At the falling limb, some sediment sources are connected late to the channel network and induce a counter-clockwise partial hysteresis loop. Thus, low energy dissipation allows the mobilization of significant quantities of sediment at the initiation of the rising and at the ending of the falling limb of the hydrograph.

In this case, none of the phases show a mostly production of sediment from the channel network. Consequently, none functions represent the sediment derived from the channel network.

However, between the low discharge, Q_0, recorded at the initiation of the flood event and $Q_{\max}$ the maximum discharge, we can assume that the concentration relative to river transport capacity increases linearly. The line segment joining the points [Q_0; $C(Q_0)$] and [$Q_{\max}$; $C(Q_{\max})$] can be used to estimate the sediments derived from the channel network. The line segment presented by dotted line (Fig. 2, Class IV (b)) is expressed by the function $C_5^{\mathrm{IV}}(t_j) = f_{\mathrm{IV}5}(Q_j)$. The component Y_{S1} is obtained from Eq. (2) with $f_{\mathrm{IV}5}$ replacing $f_{\mathrm{I}1}$.

2.4.5. Classes V and VI: single line plus one loop, clockwise (V) or anticlockwise (VI)

The single line plus loop relations combine Class I with Class II or III. C is increasing and decreasing in direct synchronization with Q during the first/last phases. Class V denotes single line plus one positive loop occurring during the rising limb. During the flood, concentration peaks before water discharge (Fig. 2, Class V (b)). Another case occurs when a counter-clockwise is observed during the falling limb of the hydrograph, when the concentration peaks after water discharge (Fig. 2, Class VI (b)).

A similar reasoning supports the distinction between Y_{S1} and Y_{S2} components shown for both cases. The sediments sampled during the first and last phases are assumed to derive from the channel network and correspond to the "base-load" single stage of the hydrograph, assumed to derive from the channel network (Fig. 2, Class V and Class VI). The model curve representing this stage is denoted $C^{\mathrm{V}}_{1\&4}(t_j) = f_{\mathrm{V}1\&4}(Q_j)$ and $C^{\mathrm{VI}}_{1\&4}(t_j) = f_{\mathrm{VI}1\&4}(Q_j)$ for Class V and Class VI, respectively.

The functions $f_{\mathrm{V}1\&4}(Q)$ and $f_{\mathrm{VI}1\&4}(Q)$ extended to all discharge measurements spanning the flood event allow to evaluate the Y_{S1} component.

2.4.6. Class VII: single line plus several loops

Sometimes, the relationship between sediment concentration and discharge is complex and exhibits single line plus several loops occurring either during the rising limb, the falling limb of the hydrograph, or during both. Such events constitute Class VII. Each loop is part of clockwise or counter-clockwise hysteresis distinguished by two stages. Like Classes V and VI, sediments sampled apart of these stages are considered as comprising a same "stage" denoted $C^{\mathrm{VII}}(t_j) = f_{\mathrm{VII}}(Q_j)$ and are assumed to derive from the channel network. The function $f_{\mathrm{VII}}(Q)$ extended to all flood discharge enables us to estimate the Y_{S1} component.

3. Results

The C–Q relationship was developed for each flood event and the main statistics like the form of hysteresis, Y_S, Y_{S1} and Y_{S2} contributions are reported in Table 1.

3.1. Annual and seasonal variability of liquid and solid discharges

The total water yield during flood events over the study period (1973–2004) was 354 hm^3, yielding a mean annual water volume of 11.4 hm^3. The annual floods of maximum flow have drained 68% of the total. Even if the water drained by these flood events show a slight downward trend (Fig. 3a), a significant upward trend appeared for the corresponding maximum peak discharge (Fig. 3-b), which varied between 0.7 and 272.6 m^3 s^{-1}.

Sediment flux estimated for the whole floods recorded during the study period (1973–2004) was estimated at 2711 × 10^3 tonnes, giving a mean annual value of 88 × 10^3 tonnes, which corresponded to a sediment yield of 343 t km^{-2} yr^{-1}. The annual suspended sediment production was shown to vary dramatically giving a very high coefficient of variation of 210%. Further, the high value of the skewness coefficient of 3.7 confirmed that sediment yield for a few years experienced extreme values. Indeed, the sediment output in 1990/1991 corresponded to more than 34% of the whole sediment output during the 31-years floods. The two biggest floods in terms of sediment flux (in spring from 3/13/1991 and in autumn from 10/5/2001) brought 39.6% of the total, and the seven main floods (i.e. 5% of all the floods recorded during the study period) carried 71% of the total. The annual floods of maximum sediment delivery have drained 64.5% of water and transported 79.8% of the total sediment yield. Sediment delivery by these most

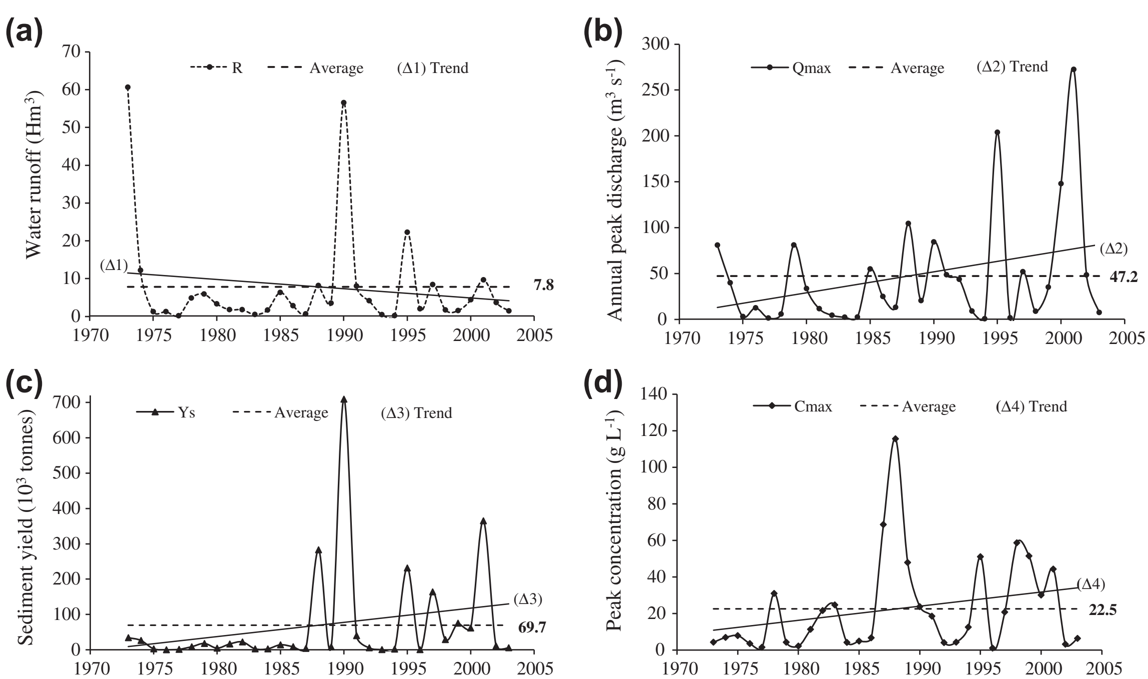

Fig. 3. Trends of annual peak floods for the period September 1973–August 2004. (a) Runoff of the annual maximum flood flows, per year, and (b) the corresponding peak discharge. (c) Sediment yield of the annual flood of maximum sediment delivery, and (d) the corresponding sediment concentration peak.

productive events revealed a strong positive trend (Fig. 3-c). The increase has accelerated at the end of the 1980s. This feature combined with the declining water supplies and prominent peak discharge has favoured high peak of suspended sediment concentration (Fig. 3d).

Within the year, the water and suspended sediment discharges also showed a high variability. Over the floods spanning the 31-years period, the water supply had averaged 16.5% in autumn and 40.5% in spring while their suspended sediment yield had averaged a quasi-equal amount, 37.9% in autumn and 35.7% in spring.

3.2. Seasonality of floods

Over the 131 floods, 51 began in autumn, 39 in winter, 28 in spring and 13 in summer. The floods were absent or short in summer (1.9 days in average), medium in autumn (6.6 days in average), and long in winter (10.7 days in average) and in spring

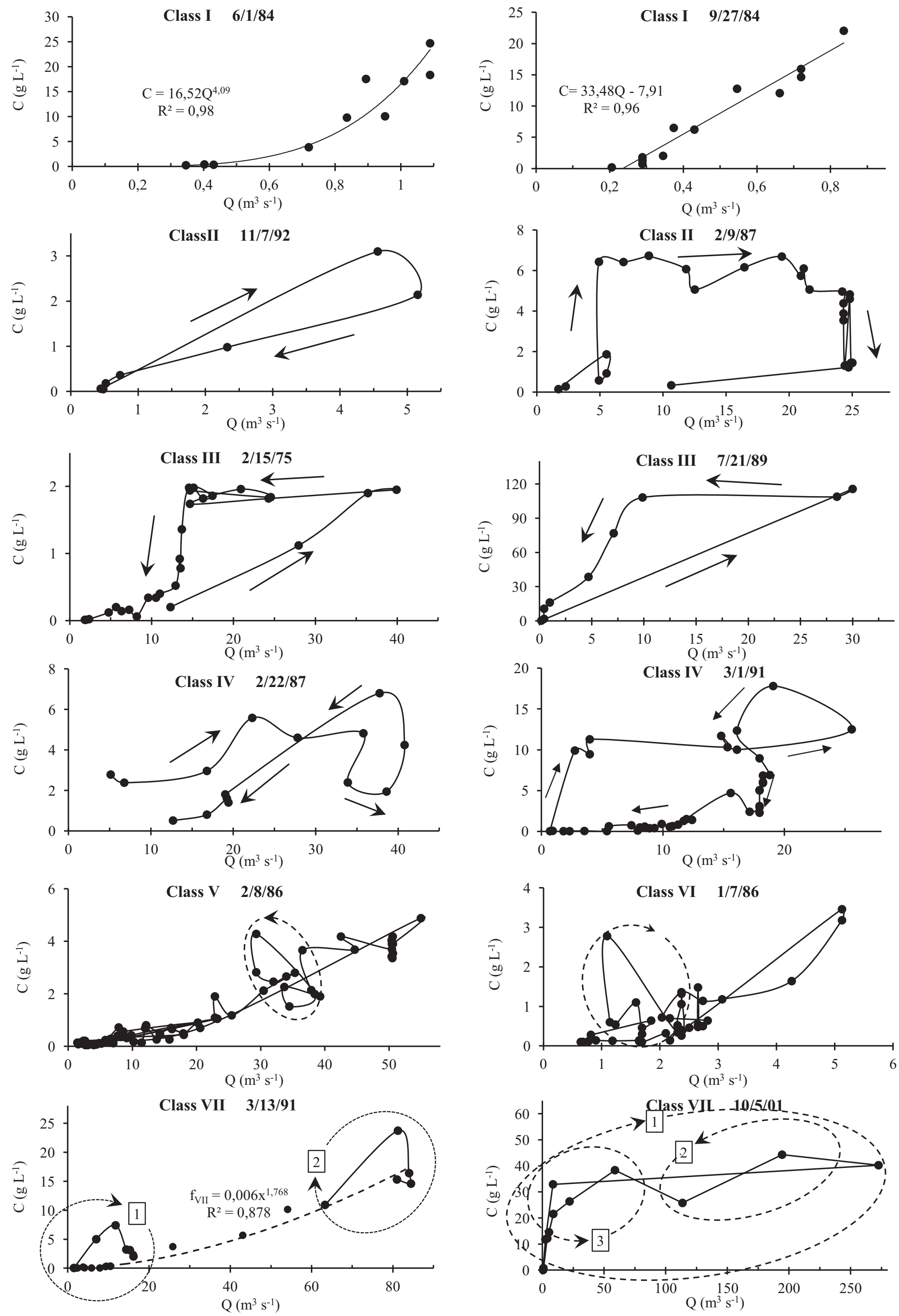

Fig. 4. Example of flood events from different classes.

(9.2 days in average). The arithmetic mean of suspended sediment concentration was the highest in summer (13.9 g L^{-1} over 13 floods), intermediate in autumn (9.6 g L^{-1} over 51 floods), low in spring (4.2 g L^{-1} over 28 floods) and lower in winter (2 g L^{-1} over 39 floods), providing a yearly average of 6.5 g L^{-1}. The highest concentration values of 106 g L^{-1} and 116 g L^{-1} occurred, respectively, in autumn 90 at the start of rainy season and in summer 89. Seasonal sediment concentration defined as the sum of sediment yield divided by the sum of water supply was low in winter (1.2 g L^{-1}), moderate in spring (6.7 g L^{-1}) and high and quasi-equal in autumn and summer, 17.6 g L^{-1} and 17.1 g L^{-1}, respectively.

Seasonal variability can be summarized as rare, short and very high turbid floods in summer, frequent, short and turbid floods in autumn, long floods in winter and spring with little turbidity in winter and moderate turbidity in spring.

3.3. Variability of flood types

The mean annual total duration of flood events was 7.8% i.e. 28.5 days per year. The annual average number of floods was four. The form of the hydrograph depended on the temporal structure of the rain storm and on its period of occurrence.

Only 18.3% of the floods were of Class VII; however, they produced 53.3% of the sediment yield. Half of the floods were either in Class II (37 of 131 floods, i.e. 28.2%) or III (31 over 131, i.e. 23.7%), and produced 15.0% and 19.4% of the total sediment yield, respectively. The 17.6% of Class IV floods produced 7.6% of sediment yield, while Classes I, V and VI represented together 12.2% (16) of the floods and brought only 4.4% of sediment (120.1×10^3 tonnes).

The short and turbid floods occurring early in the rainy season (i.e. in autumn) were mainly clockwise (14 over 51) or anticlockwise (13 over 51). But, Class VII floods represented 36.6% of the seasonal sediment yield, while Classes II and III brought 34.4% and 18.4%, respectively. The flood of 5th October 2001 (the second in terms of sediment flux) showed a complex form of Class VII and carried 13.5% of the total sediment flux (i.e. 35.6% of the cumulated seasonal sediment flux over the 31-years of study).

In winter, 16 floods over 39 (i.e. 41%) were of Class II and brought 24.6% of seasonal sediment yield, while the 7 Class VII floods brought 31.4% and the 6 Class IV floods brought 27.6%. The biggest flood was of Class VII and produced 25.2% of the seasonal cumulated sediment flux over 31-years, but only 1.3% of the total sediment flux.

In spring, one third of floods were of Class VII and the remaining were of Classes III (7/28), II and IV (5/28 each). The Class VII spring floods represented 81.9% of spring sediment delivery and 29.2% of the total sediment yield during the 31-years period of study. The biggest spring flood of 13th March 1991, of Class VII, produced alone 73.4% of the cumulated seasonal flux and 26.1% of the total flux.

In summer, 46% of floods (6/13) were of Class III. These six floods brought 50.4% of the seasonal sediment contribution, while the 3 Class VII floods brought 40.4%. However, 88.6% of the seasonal sediment flux was brought by the two biggest floods: 48.7% by the Class III flood of the 21th July 1989 (10.4% of the cumulated flux over 31-years) and 39.9% by the Class VII flood of the 16th June 1996 (8.5% of the total flux).

The five biggest floods in terms of sediment flux, which represented 3.8% of flood events (5/131) but nearly 2/3 of sediment flux (64.6%), were of three classes. One occurred in spring (the biggest, which lasted 33 days), two of them occurred in autumn (which lasted 5 and 6 days), and two in summer (durations: 2 and 9 days). Class VII (three floods) was the dominating type of these five biggest floods and generated 48.1% of the total sediment yield over the 31-years period. Finally, even if Classes II and III floods are the most frequent ones (37 and 31 events, respectively), the most productive in terms of sediment are of Class VII (24 events) because they dominate for the biggest events, whatever the season.

3.4. Y_{S1} and Y_{S2} components of each flood type

Globally, the base load Y_{S1} component was high and reached 77% of the total sediment flux, the remaining 23% (Y_{S2}) deriving from hill-slopes, re-suspension of fresh fine deposits in the river bed, and bank collapse. It must be noted that apart from the two largest of floods of 3/13/91 and 10/5/2001, the base load remained significant and reached 67% of the total.

Class I floods are only supplied from base load.

For clockwise pattern (Class II floods), other sources are available. Hill-slope material, fresh sediment deposit and/or bank caving contributed as much as 41% of the total sediment yield. However, this percentage varies considerably from one flood to another. From global point of view, the Y_{S2} component showed high contribution when the hysteresis was pronounced like on the 9th February 1987 (Fig. 4) and the 8th September 1990 (Fig. 5) when Y_{S2} contributed with 70% and 77%, respectively. Subtle clockwise hysteresis gave smaller Y_{S2} contribution, like floods of 11/7/92 where sediment supply apart from base load was about 17%.

In counter-clockwise hysteresis (Class III), sediment yield was largely supplied from base load (89.2%). Events of Class III mainly occurred in autumn and/or later in rainy season (Table 1). The late arrival of sediments in the hydrograph may be attributed in autumn to sediment derived from the distal portions of the basin and, at the end of the wet period, to bank caving. Globally, such events lasted short time but sometimes produced large quantities of sediment, like the flood of 7/21/89 which was the third largest event in terms of sediment yield (283.1×10^3 tonnes, 98% of them being attributed to Y_{S1}).

The Class IV floods (eight-shaped) produced nearly the same sediment flux in spring (40.9% with 5 floods) and in autumn (40.3% with 11 floods). The base load contributed twice more in autumn than in spring (73% against 38%). If we consider all the Class IV floods, the contribution of the Y_{S1} and Y_{S2} components were equivalent (Table 1). A fast-contribution from sediment stored in the channel network or derived from slopes in proximity of stream-flow can be hypothesized for the first clockwise loop, whereas the anti-clockwise trend occurring near the flood peak could be referred to banks collapse.

For floods of Classes V and VI, the portion of base load was only 30%, but the total sediment flux was very small.

The floods of the complex Class VII (single-line plus at least two loops) lasted long time, on average 3% of the annual time i.e. 11 days and had moderate suspended sediment concentration (7 g L^{-1}). They evacuated more than half (53.3%) of the total sediment yield carried during the study period, the majority of which was supplied by base load (84%).

Almost a third (33.2%) of sediment derived from Y_{S2} component was brought in autumn and another third in spring (36.0%) while 20.4% was brought in summer and only 10.4% in winter. As compared to Y_{S1}, the seasonal Y_{S2} contribution was high in winter (47.2% of 136×10^3 tonnes) and low in the other seasons: 20.0% of 1027×10^3 tonnes during autumn, 23.0% of 967×10^3 tonnes in spring and 21.7% of 581×10^3 tonnes in summer.

3.5. Seasonal variability of the Y_{S1} component

On first order, the Y_{S1} component can be assumed to depend linearly on Q ($C = aQ$, see Fig. 2). The analysis of all the floods shows that the linear coefficient a significantly varied with the season. The highest seasonal average was obtained in autumn ($a = 3.08$, $n = 51$) followed by that for summer events ($a = 2.15$, $n = 13$). The

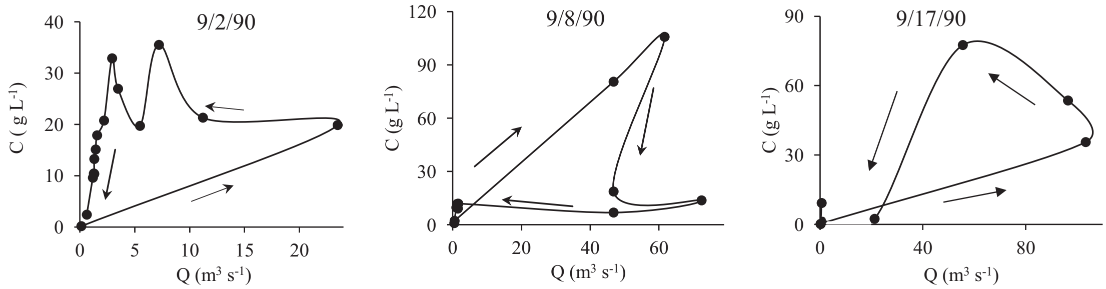

Fig. 5. Influence of timing of flood events on sediment yield: the example of three floods in September 1990.

mean coefficient for the winter and spring events was moderate ($a = 0.95$, $n = 67$). It was slightly higher for the winter events ($a = 1.03$, $n = 39$) than of those of the spring season ($a = 0.83$, $n = 28$). To estimate the base load for the largest flood of 3/13/91, the rating curves, f_{VII}, established either by linear model (with $a = 0.19$) or by power function ($C = aQ^b$) shows high coefficients of determination R^2 greater than 0.87. Consequently, with or apart from the flood of 3/13/91, the linear model which best-fits Y_{S1} showed a moderate coefficient close to 1 in winter and spring.

4. Discussion

4.1. Seasonality of flood types and sediment sources

In streams, sediment transport is mostly related to the capacity of the river to transport the available material (Ouillon and Le Guennec, 1996; van Rijn, 2005). However, the availability of hill-slopes material and the presence of significant temporary storage of sediment in the stream system cause scatter between discharge and suspended sediment load. So, the C–Q pattern is a function of the abundance of sediment furniture, and distance from active sediment sources to the basin outlet.

In Mediterranean environments such as in northwest of Algeria, where sediment transport is high, the question arises as to how significant and variable is the base load. This study conducted in the Wadi Sebdou watershed over a 31-years period of record brought partial answers. In average, 77% of sediment yield was attributed to base load. The Y_{S2} component showed seasonal variations associated to different types of floods.

In autumn, high suspended sediment discharge was linked to a large contribution of different sediment sources within the catchment area (like in September 1990, see Fig. 5). The high suspended sediment concentration was related to intense convective rain cell and to flushing of sediment accumulated during the dry summer period with low soil moisture, poor vegetation and high wind erosion (Megnounif et al., 2007). The autumn surface runoff washed out the hill-slopes and carried the fine particles (silt/clay) and organic matter produced in.

The most frequent forms of floods observed in autumn were clockwise (14/51) and counter-clockwise (13/51). Allen and Peterson (1981) reported that early flood event exhibiting counter-clockwise hysteresis in small basin was very seldom. However, the early flood events occurring in Wadi Sebdou showed counter-clockwise hysteresis 8 years over 31. Similar finding was observed in the Wadi Wahrane basin in Algeria (Benkhaled and Remini, 2003a). One reason to explain this shape is that the northern part of the basin (the closest to the gauging station) with well-developed forest cover (Bouanani, 2004) provides fewer sources of sediments in comparison with the floodplain or south slopes where there is more afforestation.

Clockwise hysteresis may be related to the availability of hill-slope sediments rapidly transported to the channel or by remobilization of fresh deposits in the channel system (Walling and Webb, 1981). Appreciable quantities of sediment deposited under low flow conditions may be available to subsequent flood events for transport within the channel. This phenomenon is produced when one flood occurs immediately after another and is enhanced during short floods like in autumn. During the falling stage of short anti-clockwise floods, river capacity rapidly decreases, sediment settles, making fresh deposit available for the next flood event. This was clearly illustrated on the successive flood events which occurred in September 1990 (Fig. 5) and exhibited alternate negative (counter-clockwise) and positive (clockwise) hysteresis. The second event (flood of 9/8/90; Fig. 5) exhibited large clockwise hysteresis. The importance of the onset of this hysteresis mainly related to the abundance of sediments available for transport, including sediments deposited during the receding stage of the previous flood event. Indeed, the high slope observed during the falling stage of the prior hydrograph (flood of 9/2/90) implies that a large amount of fresh (and thus none consolidated) sediment was stored in the channel network at this time. In contrast, the low slope of the falling stage in the second event suggests that concentration remained at a low level at the end of the flood, so the conditions favourable for sedimentation in the channel were probably lacking. That is why during the third event (flood of 9/17/90), which occurred short while after the second one, the sediment concentration could not peaked on the rising stage of the hydrograph but produced a counter-clockwise hysteresis.

The Y_{S2} component of the sediment yield was much higher during clockwise floods (41%) than during anticlockwise floods (11%) since many particles which are eroded during an anticlockwise flood (especially during the falling stage) settle before reaching the gauging station, while re-suspended particles cross the gauging station during the rising stage of a clockwise flood.

During the wet period (winter and spring), the seven classes of hydrographic events were observed in the Wadi Sebdou attesting sequential contribution of multiple and distinct sediment sources. The most common C–Q relationships exhibited hysteresis in the form of clockwise, especially in winter when 16 over 39 floods were clockwise, or complex form as single curve plus several loops, in spring. The complexity of the floods in the wet period resulted from the variability of rainfall within long lasting events, each sub-event inducing a sub-loop. The wet period was also characterized by moderate flood events exhibiting negative hysteresis (12 over 67 of winter-spring events) or sub-loops. This season corresponds to large groundwater contribution. Under high moisture conditions, the mechanisms of erosion operate locally. Saturation areas near channel network may function as storing tanks. At the receding stage of the hydrograph, bank caving provides a significant source of sediments easily carried out by the stream. However, their contribution was lower than the amount of sediment yielded in the hydrographical network. So, while the mechanisms generating suspended sediments are diverse, the amounts of suspended sediment supplied during the spring season were as much important as that produced in autumn inducing the same contribution of base load.

The complex C–Q relationship of Class VII indicates that the major amount of sediment has been flushed through the system and occasionally new sediment sources are available during the event. This was the case during large flood events and particularly during the 33-days long flood of 3/13/91 where base load was estimated by using a power model $C = aQ^b$, as classically encountered in larger basins. Such strong dependence of C on Q occurs in a system that derives most of its sediment from entrainment of bed material (Bagnold, 1966), and transports a smaller proportion of wash-load. This observation is also consistent with Roose et al. (1998) who explained that, during large and prolonged flood events, soils saturate and that significant erosion may results in the development of major erosional gullies on the hillside, the gullies being considered as the extension of the hydrographical network.

4.2. Regional and climate impacts on sediment transport

During the 31-years period of study, the suspended sediment supply to the outlet was 2.7×10^6 tonnes of which 77% was produced in the hydrographical network. The huge percentage confirmed the importance of hydrographical network erosion in the sediment production system and corroborated the findings of Heusch and Millies-Lacroix (1971) in Maghreb Mountains. Similar result was attested by Vanmaercke et al. (2010) working in the northern Ethiopian highlands.

The 31-years record of floods in the Wadi Sebdou showed an increasing trend in annual peak flows, annual maximum discharges and concentrations (Fig. 3). The trend in water runoff may be biased by a single value – the maximum value – measured for the first year of the study period. However, there is evidence of the increase of peak flows and sediment delivery from the end of the 1980s. After 1988, the sediment flux carried by the annual flood of maximum sediment delivery has doubled in comparison with the entire study period. A similar trend was observed on the Wadi Abd by Achite and Ouillon (2007) who also pointed that the sediment delivery was highly correlated to the irregularity of flows (characterized by its standard deviation). Vachtman et al. (2012) reported a recent increase of flood frequency in the Qishon River basin in the eastern Mediterranean area as well and considered it as the primary forcing factor in the rate of sediment supply. These finding corroborate recent studies which provide clear evidence of significant changes in the hydrology of Mediterranean Rivers in response to global changes, since interactions between mid-latitude and tropical processes may be highly affected by minor modifications of the general circulation (Giorgi and Lionello, 2008). The strong summer–winter rainfall contrast being the major characteristic of the Mediterranean climate, the present trend toward drier and warmer conditions is likely responsible for the general reduction observed in freshwater delivery around the Mediterranean Sea (Ludwig et al., 2009). These two papers also underlined the substantial fine scale structure of the climate response to the forcing of the complex topography of the region.

In dry lands, several factors and parameters can combine and favour high erosion (Langbein and Schumm, 1958; Colombani et al., 1984; Scott, 2006). At the beginning of the rainy season, floodplains are generally poor in vegetation and soils are usually more compacted. Consequently, rains exert an important impact on the exposed soils, including splashing of soil particles and promoting high peak flows as rainwater does not infiltrate into soil instantly. Moreover, the rapid wetting of the desiccated soil causes the aggregates to disintegrate which increases the susceptibility to soil erosion (Martínez-Mena et al., 1998; Barthès and Roose, 2002). For these reasons, overland flow forms the major component of basin runoff and results in important weathering in hydrographical network. Because the rain-showers are often intense and local, small portion of sediment derives from hill-slopes. The contribution becomes important only when rainfall interests the whole of the catchment.

During the wet season, river capacity mainly governs sediment fluxes. The soil moisture is a main factor steering the processes of sediment yield where physical and chemical processes make-up erosion. When soils are close to saturation, water erosion consists of mass movements on the steep slopes where the soil is thin and the collapse of stream banks. Following the example of Mediterranean's soil, in the Wadi Sebdou basin, the richness in soluble salts favours tunnel erosion. A gully remains when surface soil collapse into tunnel. Considering the extension of the hydrographical network, the gullies confer high drainage density on the catchment basin, maximizing the opportunity for both water and eroded soil to reach the channel network (Heusch, 1982; Probst and Amiotte-Suchet, 1992; Scott, 2006; Vanmaercke et al., 2010). The studies conducted by Roose (1991) in northern Algeria and Heusch (1970) in the Rif Mountains of Morocco reveal that gully sediment yields were significantly greater than hill-slope sediment yields. Tunnel erosion could likely explain multimodality of many floods but this assumption needs to be assessed by future experiments.

4.3. Methodology

A hydrograph separation method used by Etchanchu and Probst (1986) was applied by Megnounif et al. (2003) to quantify the "Y_{S1} component" in the Wadi Sebdou. For the period from September 1988 to August 1993, this component was evaluated to be much lower (38%) than the estimation (77% over the 31-years of study, 88% over 1988–1993) in the present study because the two methods are totally different. In fact, the two methods provide different "Y_{S1}" parameters. Indeed, the identification of sediment sources in the hydrograph separation method is based solely on the flow characteristics and does not take into account the fluctuation of C. While it was shown in this present study that, in most cases, appreciable quantities of sediments are derived from new sediment sources which are active during the recession of the hydrograph, the hydrograph separation method assumes that during delayed flow, sediments exclusively derived from the hydrographical network.

5. Conclusions

The new graphical method applied in this paper enabled us to: (1) elucidate the relationship between C–Q hysteresis types and sediment sources within the river basin, using models and field examples; (2) provide a simple graphical explanation for each type; and (3) estimate the contribution of distinct sediment sources at event scale. Its application allowed to better understand the dynamics of sediment fluxes during the floods which are a major concern to provide solutions to reduce their impacts. In the light of this study, the majority of sediment delivered at the outlet of the basin was derived from hydrographical network which contributed to about 77% of total sediment yield throughout the 31-years of study.

The ratio of the Y_{S1} contribution varied within a year. The short and turbid floods, rare in summer and frequent in autumn, were mainly of Classes II and III. Their short duration is favourable to re-suspension and settling during the rising and falling stages. Several pairs of successive anticlockwise then clockwise floods were observed. At the start of the rainy season, hill-slopes material was also considered as a major contributor to sediment discharge when rainfall interested the whole of the catchment. This explained that more than 33% of the Y_{S2} component along the year was transported in autumn, while Y_{S1} component accounted 30% of its yearly contribution. The long and low turbid floods in winter and spring, rare in winter and frequent in spring, were mainly of Classes II and VII. The main sediment source was the base load induced by river capacity. The long duration of floods did not allow high settling of particles in the river bed. These floods were likely more complex because, being longer, they experienced intra-event variability in rainfall, because of pulse effects like bank caving, and because of the impact of underground water inputs. However, these effects induced lower sediment fluxes than those in autumn related to hill-slopes or re-suspension of fresh deposits.

The most frequent floods were clockwise or anticlockwise (52% of floods) but brought only 34% of the total sediment flux. The 18% of the floods which were single valued plus at least two loops produced more than 53% of the sediments, mainly supplied by base load (84%).

Intra-annual variability was very high. Over 31-years, the five biggest floods cumulated 64% of the total sediment flux and were of three classes, the most complex floods being dominant. Apart from these five biggest flood events, the Y_{S1} component represented 53%. The biggest floods favoured base load as compared to the smallest ones.

This study also evidenced hydroclimatic changes in the Wadi Sebdou, characterized by increasing annual peak flows and associated sediment deliveries during the study period. However, their long-term evolution superimpose to the cyclicity of humid and dry periods which occurs in the Mediterranean basin in intervals of about 20 years (Ludwig et al., 2009). Sediment dynamics and its budget at the overall Mediterranean basin thus require more extensive monitoring of numerous events, especially in many medium and small (<10,000 km^2) basins, which drain 16% of its watershed but supply almost 70% of its water load (Poulos, 2011).

Acknowledgments

The authors thank the National Agency of Hydrologic Resources [ANRH], the Algerian agency in charge of stream gauging, which provided all water flows and sediment concentrations data. They also thank two anonymous reviewers and the associate editor for their comments and suggestions.

References

Achite, M., Meddi, M., 2005. Variabilité spatio-temporelle des apports liquide et solide en zone semi-aride. Cas du bassin versant de l'oued Mina (nord-ouest algérien). Rev. Sci. Eau 18, 37–56.
Achite, M., Ouillon, S., 2007. Suspended sediment transport in a semiarid watershed, Wadi Abd, Algeria (1973–1995). J. Hydrol. 343, 187–202.
Allen, P.B., Peterson, D., 1981. A study of the variability of suspended sediment measurements. Erosion and Sediment Transport Measurements, vol. 133. IAHS Publication, pp. 203–211.
Asselman, N.E.M., 1999. Suspended sediment dynamics in a large drainage basin: the River Rhine. Hydrol. Proc. 13, 1437–1450.
Bača, P., 2008. Hysteresis effect in suspended sediment concentration in the Rybárik basin, Slovakia. Hydrol. Sci. J. 53 (1), 224–235.
Bagnold, R.A., 1966. An Approach to the Sediment Transport Problem form General Physics. U.S. Geological Survey Professional Paper, 422-J.
Barthès, B., Roose, E., 2002. Aggregate stability as an indicator of soil susceptibility to runoff and erosion; validation at several levels. Catena 47, 133–149.
Benkhaled, A., Remini, B., 2003a. Variabilité temporelle de la concentration en sédiments et phénomène d'hystérésis dans le bassin de l'Oued Wahrane (Algérie). J. Sci. Hydrol. 48 (2), 243–255.
Benkhaled, A., Remini, B., 2003b. Analyse de la relation de puissance: débit solide – débit liquide à l'échelle du bassin versant de l'Oued Wahrane (Algérie). Rev. Sci. Eau 16 (3), 333–356.
Bouanani, A., 2004. Hydrologie, transport solide et modélisation. Etude de quelques sous bassins de la Tafna (NW–Algérie). Ph.D. Thesis, Tlemcen University, Algeria, 250p.
Bourouba, M., 1998. Contribution à l'étude de l'érosion et des transports solides de l'Oued Medjerda supérieur (Algérie orientale). Bull. Réseau Érosion 18, 76–97.
Colombani, J., Olivry, J.C., Kallel, R., 1984. Phénomènes exceptionnels d'érosion et de transport solide en Afrique aride et semi-aride. Challenges in African Hydrology and Water Ressources, vol. 144. IAHS Publication, pp. 295–300.
de Boer, D.H., Campbell, I.A., 1989. Spatial scale dependence of sediment dynamics in a semi-arid badland drainage basin. Catena 16, 277–290.
Djeziri, L., 1998. Envasement des barrages, mobiliser le maximum de capacité. Revue Symbiose 2, 18–21.
Etchanchu, D., Probst, J.L., 1986. Erosion et transport de matières en suspension dans un bassin versant en région agricole. Méthode de mesure du ruissellement superficiel, de sa charge et des deux composantes du transport solide dans un cours d'eau. C. R. Acad. Sci. Paris série II 302 (17), 1063–1067.
Fang, N.F., Shi, Z.H., Li, L., Jiang, C., 2011. Rainfall, runoff, and suspended sediment delivery relationships in a small agricultural watershed of the Three Gorges area, China. Geomorphology 135 (1–2), 158–166.
Gellis, A.C., 2013. Factors influencing storm-generated suspended-sediment concentrations and loads in four basins of contrasting land use, humid-tropical Puerto Rico. Catena 104, 39–57.
Giorgi, F., Lionello, P., 2008. Climate change projections for the Mediterranean region. Global Planet. Change 63 (2–3), 90–104.
Ghenim, A., Seddini, A., Terfous, A., 2008. Variation temporelle de la dégradation spécifique du bassin versant de l'Oued Mouilah (nord-ouest Algérien). Hydrol. Sci. J. 53 (2), 448–456.
Ghenim, A., Terfous, A., Seddini, A., 2007. Etude du transport solide en suspension dans les régions semi-arides méditerranéennes: cas du bassin versant de l'oued Sebdou (nord-ouest algérien). Sécheresse 18 (1), 39–44.
Ghorbal, A., Claude, J., 1977. Mesure de l'envasement dans les retenues de sept barrages en Tunisie: estimation des transports solides, vol. 122. IAHS Publication, pp. 219–232.
Gregory, K.J., Walling, D.E., 1973. Drainage Basin Form and Process. Edward Arnold, London, 458 p.
Heidel, S.G., 1956. The progressive lag of sediment concentration with flood waves. Trans. Am. Geophys. Union 37, 56–66.
Heusch, B., 1970. L'érosion du Pré-Rif – Une étude quantitative de l'érosion hydraulique dans les collines marneuses du Pré-Rif occidental. Ann. Recherches Forestières de Maroc 12, 9–176.
Heusch, B., 1982. Etude de l'érosion et des transports solides en zone semi aride. Recherche bibliographique sur l'Afrique du Nord. Project RAB/80/04/PNUD.
Heusch, B., Millies-Lacroix, A., 1971. Une méthode pour estimer l'écoulement et l'érosion dans un bassin. Application au Maghreb. Mine et Géologie 33, 21–39, Rabat, Maroc.
Hudson, P.F., 2003. Event sequence and sediment exhaustion in the lower Panuco basin, Mexico. Catena 52, 57–76.
Jansson, M.B., 2002. Determining sediment source areas in a tropical river basin, Costa Rica. Catena 47, 63–84.
Kassoul, M., Abdelgader, A., Belorgey, M., 1997. Caractérisation de la sédimentation des barrages en Algérie. Rev. Sci. Eau 3, 339–358.
Khanchoul, K., Jansson, M.-B., 2008. Sediment rating curves developed on stage and seasonal means in discharge classes for the Mellah Wadi, Algeria. Geogr. Ann. 90A (3), 227–236.
Klein, M., 1984. Anti clockwise hysteresis in suspended sediment concentration during individual storms: Holbeck catchment; Yorkshire, England. Catena 11, 251–257.
Langbein, W.B., Schumm, S.A., 1958. Yield of sediments in relation to mean annual precipitation. Trans. Am. Geophys. Union 39, 1076–1084.
Lecce, S.A., Pease, P.P., Gares, P.A., Wang, J., 2005. Seasonal controls on sediment delivery in a small coastal plain watershed, North Carolina, USA. Geomorphology 73, 246–260.
Ludwig, W., Dumont, E., Meybeck, M., Heussner, S., 2009. River discharges of water and nutrients to the Mediterranean sea: major drivers for ecosystem changes during past and future decades? Prog. Oceanogr. 80, 199–217.
Martínez-Mena, M., Williams, A.G., Ternan, J.L., Fitzjohn, C., 1998. Role of antecedent soil water content on aggregates stability in a semi-arid environment. Soil Till. Res. 48, 71–80.
Megnounif, A., Bouanani, A., Terfous, A., Baba Hamed, K., 1999. Distributions statistiques de la pluviométrie et mise en évidence de l'influence du relief (cas des Monts de Tlemcen, Nord Ouest Algérien). Sci. Technol. 12, 77–80.
Megnounif, A., Terfous, A., Bouanani, A., 2003. Production et transport des matières solides en suspension dans le bassin versant de la Haute Tafna (Nord Ouest Algérien). Rev. Sci. Eau 16 (3), 369–380.
Megnounif, A., Terfous, A., Ghenaim, A., Poulet, J.B., 2007. Key processes influencing erosion and sediment transport in a semi-arid Mediterranean area: the upper Tafna catchment, Algeria. Hydrol. Sci. J. 52 (6), 1271–1284.
Ouillon, S., Le Guennec, B., 1996. Modelling non-cohesive suspended sediment transport in 2D vertical free surface flows. J. Hydr. Res. 34 (2), 219–236.
Peart, M.R., Walling, D.E., 1982. Particle size characteristics of fluvial suspended sediment. Recent Developments in the Explanation and Prediction of Erosion and Sediment Yield, vol. 137. IAHS Publication, pp. 397–407.
Picouet, C., Hingray, B., Olivry, J.C., 2001. Empirical and conceptual modelling of the suspended sediment dynamics in a large tropical African river: the upper Niger river basin. J. Hydrol. 250, 19–39.
Poulos, S.E., 2011. An insight to the fluvial characteristics of the Mediterranean and Black sea watersheds. In: Lambrakis, N., Stournaras, G., Katsanou, K. (Eds.), Advances in the Research of Aquatic Environment. Springer, pp. 191–198.
Probst, J.L., Amiotte-Suchet, P., 1992. Fluvial suspended sediment transport and mechanical erosion in the Maghreb (North Africa). Hydrol. Sci. J. 37, 621–637.

Probst, J.L., Bazerbachi, A., 1986. Transport en solution et en suspension par la Garonne supérieure. Sci. Géol. Bull. 39 (1), 79–98.

Robinson, A.R., 1977. Relationships between soil erosion and sediment delivery. Erosion and solid matter transport in inland waters. IAHS Bull. 122, 159–167.

Roehl, J.W., 1962. Sediment Source Areas, Delivery Ratios, and Influencing Morphological Factors, vol. 59. IAHS Publication, pp. 202–213.

Roose, E., 1991. Conservation des sols en zones méditerranéennes – Synthèse et proposition d'une nouvelle stratégie de lutte antiérosive: la CGES. Cahiers ORSTOM, série Pédologie, XXVI 2, 145–181.

Roose, E., Arabi, M., Chebbani, M., Mazour, M., Morsli, B., 1998. Les montagnes méditerranéennes d'Algérie. Impact de l'intensification de l'agriculture de montagne sur l'environnement et les revenues. ORSTOM Actualité Spécial Erosion 56, 26–27.

Rovira, A., Batalla, R.J., 2006. Temporal distribution of suspended sediment transport in a Mediterranean basin: the lower Tordera (NE Spain). Geomorphology 79 (1–2), 58–71.

Seeger, M, Errea, M.P., Beguería, S., Arnáez, J., Martí, C., Garcıa-Ruiz, J.M., 2004. Catchment soil moisture and rainfall characteristics as determinant factors for discharge/suspended sediment hysteretic loops in a small headwater catchment in the Spanish Pyrenees. Journal of Hydrology 288 (3–4), 299–311..

Scott, S., 2006. Predicting Sediment Transport Dynamics in Ephemeral Channels: A Review of Literature. ERDC/CHL CHETN-VII-6. U.S. Army Engineer Research and Development Center, Vicksburg, MS. <http://chl.erdc.usace.army.mil/chetn>.

Terfous, A., Megnounif, A., Bouanani, A., 2001. Study of the suspended load at the river Mouilah (north west Algeria). Rev. Sci. Eau 14 (2), 173–185.

Uys, M.C., O'Keeffe, J.H., 1997. Simple words and fuzzy zones: early directions for temporary river research in South Africa. Environ. Manage. 21 (4), 517–531.

van Rijn, L.C., 2005. Principles of Sediment Transport in Rivers, Estuaries and Coastal Seas. Aqua Publications.

Vanmaercke, M., Zenebe, A., Poesen, J., Nyssen, J., Verstraeten, G., Deckers, J., 2010. Sediment dynamics and the role of flash floods in sediment export from medium-sized catchments: a case study from the semi-arid tropical highlands in northern Ethiopia. J. Soils Sediments 10, 611–627.

Vachtman, D., Sandler, A., Herut, B., Greenbaum, N., 2012. Dynamics of suspended sediment delivery to the eastern Mediterranean continental shelf. Hydrol. Process.. http://dx.doi.org/10.1002/hyp.9265.

Walling, D.E., Webb, B.W., 1981. The reliability of suspended load data. Erosion and Sediment Transport Measurement, vol. 133. IAHS Publication, pp. 177–194.

Walling, D.E., Webb, B.W., 1982. Sediment Availability and Prediction of Storm-period Sediment Yields, vol. 137. IAHS Publication, pp. 327–337.

Williams, G.P., 1989. Sediment concentration versus water discharge during single hydrologic events in rivers. J. Hydrol. 111, 89–106.